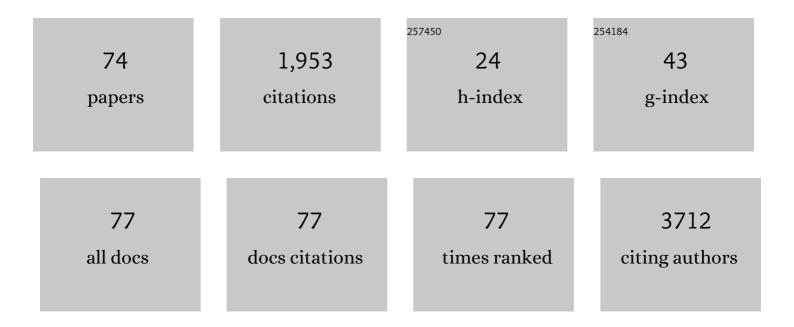
Jeffery Aguiar

List of Publications by Year in descending order

Source: https://exaly.com/author-pdf/527056/publications.pdf Version: 2024-02-01



IFFFFDY ACHIAD

#	Article	IF	CITATIONS
1	Structure and radiation response of anion excess bixbyite Gd2Ce2O7. Physical Review Materials, 2022, 6, .	2.4	3
2	Integrating atomistic simulations and machine learning to design multi-principal element alloys with superior elastic modulus. Journal of Materials Research, 2022, 37, 1497-1512.	2.6	7
3	Advances in the electron diffraction characterization of atomic clusters and nanoparticles. Nanoscale Advances, 2021, 3, 311-325.	4.6	13
4	Structureâ€Induced Stability in Sinuous Black Silicon for Enhanced Hydrogen Evolution Reaction Performance. Advanced Functional Materials, 2021, 31, 2008888.	14.9	5
5	Solar wind contributions to Earthâ \in ^M s oceans. Nature Astronomy, 2021, 5, 1275-1285.	10.1	22
6	Assessing the solid-state kinetics and behavior for uranium-free Pu-12Am–40Zr alloys at 973†K. Journal of Alloys and Compounds, 2020, 817, 152735.	5.5	1
7	Densification of graphite under high pressure and moderate temperature. Materials Today Communications, 2020, 22, 100821.	1.9	2
8	Crystallographic prediction from diffraction and chemistry data for higher throughput classification using machine learning. Computational Materials Science, 2020, 173, 109409.	3.0	27
9	Cadmium Selective Etching in CdTe Solar Cells Produces Detrimental Narrow-Gap Te in Grain Boundaries. ACS Applied Energy Materials, 2020, 3, 1749-1758.	5.1	6
10	High Throughput Crystal Structure Classification. Microscopy and Microanalysis, 2020, 26, 10-12.	0.4	1
11	Bringing nuclear materials discovery and qualification into the 21st century. Nature Communications, 2020, 11, 2556.	12.8	18
12	Freestanding Thinâ€Films: Waterâ€Assisted Liftoff of Polycrystalline CdS/CdTe Thin Films Using Heterogeneous Interfacial Engineering (Adv. Mater. Interfaces 14/2019). Advanced Materials Interfaces, 2019, 6, 1970095.	3.7	0
13	Observation and Implications of Composition Inhomogeneity Along Grain Boundaries in Thin Film Polycrystalline CdTe Photovoltaic Devices. Advanced Materials Interfaces, 2019, 6, 1900152.	3.7	5
14	In-situ Ion Irradiation and Recrystallization in Highly Structured Materials. Microscopy and Microanalysis, 2019, 25, 1572-1573.	0.4	1
15	Structural and Compositional Properties of Recrystallized CdS/CdTe Thin-Films Grown on Oxidized Silicon Substrates. Microscopy and Microanalysis, 2019, 25, 2166-2167.	0.4	1
16	Merging Deep Learning, Chemistry, and Diffraction for High-Throughput Material Structure Prediction. Microscopy and Microanalysis, 2019, 25, 168-169.	0.4	0
17	Localized corrosion of low-carbon steel at the nanoscale. Npj Materials Degradation, 2019, 3, .	5.8	31
18	Waterâ€Assisted Liftoff of Polycrystalline CdS/CdTe Thin Films Using Heterogeneous Interfacial Engineering. Advanced Materials Interfaces, 2019, 6, 1900300.	3.7	7

JEFFERY AGUIAR

#	Article	IF	CITATIONS
19	Dual Protection Layer Strategy to Increase Photoelectrode–Catalyst Interfacial Stability: A Case Study on Black Silicon Photoelectrodes. Advanced Materials Interfaces, 2019, 6, 1802085.	3.7	13
20	Unbiased solar H ₂ production with current density up to 23 mA cm ^{â^'2} by Swiss-cheese black Si coupled with wastewater bioanode. Energy and Environmental Science, 2019, 12, 1088-1099.	30.8	48
21	Decoding crystallography from high-resolution electron imaging and diffraction datasets with deep learning. Science Advances, 2019, 5, eaaw1949.	10.3	81
22	Mapping carrier lifetime variations in polycrystalline CdTe thin films using confocal microscopy. , 2018, , .		1
23	A Strategy to Mitigate Grain Boundary Blocking in Nanocrystalline Zirconia. Journal of Physical Chemistry C, 2018, 122, 26344-26352.	3.1	8
24	Pioneering the Use of Neural Network Architectures and Feature Engineering for Real-Time Augmented Microscopy and Analysis. Microscopy and Microanalysis, 2018, 24, 514-515.	0.4	0
25	A graded catalytic–protective layer for an efficient and stable water-splitting photocathode. Nature Energy, 2017, 2, .	39.5	135
26	Cr incorporated phase transformation in Y2O3 under ion irradiation. Scientific Reports, 2017, 7, 40148.	3.3	6
27	In situ investigation of halide incorporation into perovskite solar cells. MRS Communications, 2017, 7, 575-582.	1.8	7
28	Thermodynamics versus kinetics of grain growth control in nanocrystalline zirconia. Acta Materialia, 2017, 136, 224-234.	7.9	38
29	Cation ratio fluctuations in Cu ₂ ZnSnS ₄ at the 20 nm length scale investigated by analytical electron microscopy. Physica Status Solidi (A) Applications and Materials Science, 2016, 213, 2392-2399.	1.8	11
30	Atomic scale understanding of poly-Si/SiO <inf>2</inf> /c-Si passivated contacts: Passivation degradation due to metallization. , 2016, , .		3
31	Plasma immersion ion implantation for interdigitated back passivated contact (IBPC) solar cells. , 2016, , .		1
32	Module degradation mechanisms studied by a multi-scale approach. , 2016, , .		7
33	In situ investigation of the formation and metastability of formamidinium lead tri-iodide perovskite solar cells. Energy and Environmental Science, 2016, 9, 2372-2382.	30.8	79
34	Revealing the semiconductor–catalyst interface in buried platinum black silicon photocathodes. Journal of Materials Chemistry A, 2016, 4, 8123-8129.	10.3	15
35	Effect of Water Vapor, Temperature, and Rapid Annealing on Formamidinium Lead Triiodide Perovskite Crystallization. ACS Energy Letters, 2016, 1, 155-161.	17.4	27
36	Combined effects of radiation damage and He accumulation on bubble nucleation in Gd2Ti2O7. Journal of Nuclear Materials, 2016, 479, 542-547.	2.7	16

JEFFERY AGUIAR

#	Article	IF	CITATIONS
37	Sodium Accumulation at Potential-Induced Degradation Shunted Areas in Polycrystalline Silicon Modules. IEEE Journal of Photovoltaics, 2016, 6, 1440-1445.	2.5	48
38	Interface Characterization of Single-Crystal CdTe Solar Cells With VOC > 950 mV. IEEE Journal of Photovoltaics, 2016, 6, 1650-1653.	2.5	10
39	Electrophobic interaction induced impurity clustering in metals. Acta Materialia, 2016, 119, 1-8.	7.9	36
40	Low-cost plasma immersion ion implantation doping for Interdigitated back passivated contact (IBPC) solar cells. Solar Energy Materials and Solar Cells, 2016, 158, 68-76.	6.2	37
41	Contrasting the Material Chemistry of Cu ₂ ZnSnSe ₄ and Cu ₂ ZnSnS _{(4–} <i>_x</i> ₎ Se <i>_x</i> Advanced Science, 2016, 3, 1500320.	11.2	13
42	Revealing Surface Modifications of Potassiumâ€Fluorideâ€Treated Cu(In,Ga)Se ₂ : A Study of Material Structure, Chemistry, and Photovoltaic Performance. Advanced Materials Interfaces, 2016, 3, 1600013.	3.7	24
43	Bubble formation and lattice parameter changes resulting from He irradiation of defect-fluorite Gd2Zr2O7. Acta Materialia, 2016, 115, 115-122.	7.9	39
44	CdTe solar cells with open-circuit voltage breaking the 1 V barrier. Nature Energy, 2016, 1, .	39.5	307
45	Tracking the Evolution of in-situ Radiochemistry with Transmission Electron Microscopy. Microscopy and Microanalysis, 2015, 21, 1747-1748.	0.4	0
46	Non-uniform Solute Segregation at Semi-Coherent Metal/Oxide Interfaces. Scientific Reports, 2015, 5, 13086.	3.3	21
47	Studying Perovskite-based Solar Cells with Correlative In-Situ Microscopy. Microscopy and Microanalysis, 2015, 21, 969-970.	0.4	11
48	Structural analysis of Gd2Ce2O7. Materials Research Society Symposia Proceedings, 2015, 1743, 7.	0.1	2
49	Structure and segregation of dopant–defect complexes at grain boundaries in nanocrystalline doped ceria. Physical Chemistry Chemical Physics, 2015, 17, 15375-15385.	2.8	33
50	Interface Energies of Nanocrystalline Doped Ceria: Effects of Manganese Segregation. Journal of Physical Chemistry C, 2015, 119, 27855-27864.	3.1	36
51	Nanoscale morphologies at alloyed and irradiated metal-oxide bilayers. Journal of Materials Science, 2015, 50, 2726-2734.	3.7	4
52	Oxidatively Stable Nanoporous Silicon Photocathodes with Enhanced Onset Voltage for Photoelectrochemical Proton Reduction. Nano Letters, 2015, 15, 2517-2525.	9.1	80
53	Irradiation-induced formation of a spinel phase at the FeCr/MgO interface. Acta Materialia, 2015, 93, 87-94.	7.9	8
54	Solute redistribution and phase stability at FeCr/TiO2â^' interfaces under ion irradiation. Acta Materialia, 2015, 89, 364-373.	7.9	9

JEFFERY AGUIAR

#	Article	IF	CITATIONS
55	Probing battery chemistry with liquid cell electron energy loss spectroscopy. Chemical Communications, 2015, 51, 16377-16380.	4.1	25
56	Mapping strain modulated electronic structure perturbations in mixed phase bismuth ferrite thin films. Journal of Materials Chemistry C, 2015, 3, 1835-1845.	5.5	14
57	Role of the interface on radiation damage in the SrTiO3/LaAlO3 heterostructure under Ne2+ ion irradiation. Journal of Applied Physics, 2014, 115, .	2.5	10
58	Defect interactions with stepped CeO2/SrTiO3 interfaces: Implications for radiation damage evolution and fast ion conduction. Journal of Chemical Physics, 2014, 140, 194701.	3.0	21
59	Orientation-specific amorphization and intercalated recrystallization at ion-irradiated SrTiO ₃ /MgO interfaces. Journal of Materials Research, 2014, 29, 1699-1710.	2.6	14
60	Linking Interfacial Step Structure and Chemistry with Locally Enhanced Radiationâ€Induced Amorphization at Oxide Heterointerfaces. Advanced Materials Interfaces, 2014, 1, 1300142.	3.7	25
61	Effect of helium irradiation on Ti3AlC2 at 500°C. Scripta Materialia, 2014, 77, 1-4.	5.2	51
62	Thermal Expansion, Heat Capacity, and Thermal Conductivity of Nickel Ferrite (NiFe ₂ O ₄). Journal of the American Ceramic Society, 2014, 97, 1559-1565.	3.8	51
63	Termination chemistry-driven dislocation structure at SrTiO3/MgO heterointerfaces. Nature Communications, 2014, 5, 5043.	12.8	39
64	Hidden one-dimensional spin modulation in a three-dimensional metal. Nature Communications, 2014, 5, 4218.	12.8	12
65	Quantifying the low-energy limit and spectral resolution in valence electron energy loss spectroscopy. Ultramicroscopy, 2013, 124, 130-138.	1.9	13
66	SANS and TEM of ferritic–martensitic steel T91 irradiated in FFTF up to 184dpa at 413°C. Journal of Nuclear Materials, 2013, 440, 91-97.	2.7	36
67	Interfacial Ferromagnetism in <mml:math <br="" xmlns:mml="http://www.w3.org/1998/Math/MathML">display="inline"><mml:msub><mml:mi>LaNiO</mml:mi><mml:mn>3</mml:mn></mml:msub><mml:mo>/Physical Review Letters, 2013, 111, 087202.</mml:mo></mml:math>	:mø.% mn	าl:m ร ub> <mr< td=""></mr<>
68	Investigating the electronic structure of fluorite-structured oxide compounds: comparison of experimental EELS with first principles calculations. Journal of Physics Condensed Matter, 2012, 24, 295503.	1.8	2
69	Determining the Atomic Structure of [111] Tilt Grain Boundaries in Ceria. Microscopy and Microanalysis, 2012, 18, 386-387.	0.4	0
70	Atomic-Scale Imaging and Spectroscopy for <i>In Situ</i> Liquid Scanning Transmission Electron Microscopy. Microscopy and Microanalysis, 2012, 18, 621-627.	0.4	125
71	Characterization of secondary phases and other defects in CdZnTe. , 2010, , .		4
72	Electronic structure of oxide fuels from experiment and first principles calculations. Journal of Physics: Conference Series, 2010, 241, 012062.	0.4	5

#	Article	IF	CITATIONS
73	Studying the Electronic Structure of Uranium Dioxide. Microscopy and Microanalysis, 2009, 15, 1380-1381.	0.4	Ο
74	Black carbon concentrations and diesel vehicle emission factors derived from coefficient of haze measurements in California: 1967–2003. Atmospheric Environment, 2008, 42, 480-491.	4.1	64